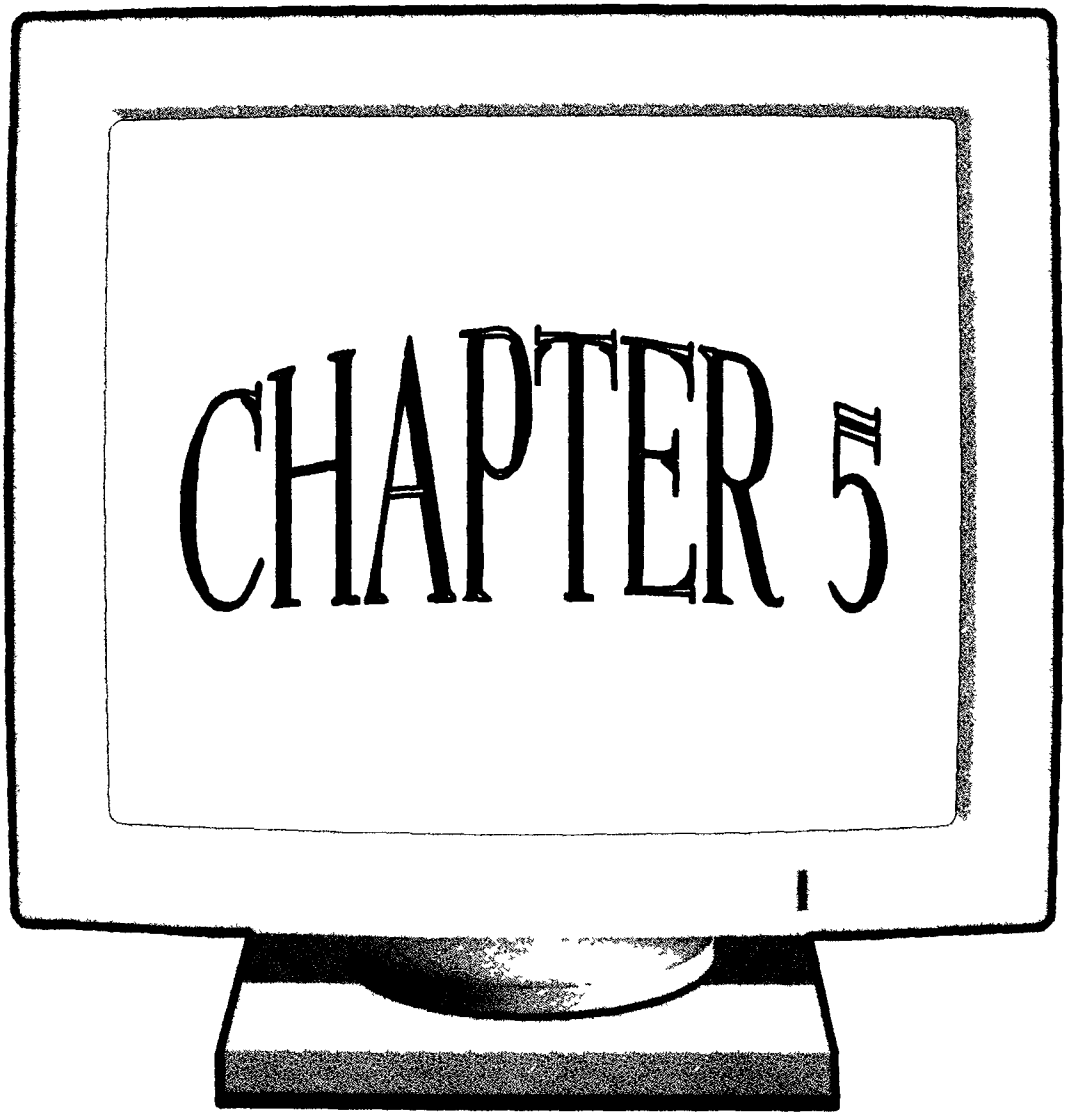
CHAPTER 5

CHAPTER 5

MODIFICATION OF PADC THROUGH ELECTRON-TARGET COLLISION

5.1. INTRODUCTION

In a passage of an initially homogenous beam of electrons through a target, the apparent straggling is pronounced by scattering of electrons into different directions, giving rise to different path-lengths of electrons traversing the same thickness of the absorber. The electrons are deflected much more readily than heavier particles by which imprecision can be introduced in measuring the thickness of the absorber needed to stop the electrons of a given energy (Beiser, 1997). When compared with heavy charged particles, fast electrons lose energy at a lower rate and follow a more torturous path through the absorbing materials. Nuclear scattering is responsible for most of the large angle deflections, although energy-loss is caused almost entirely by interactions with electrons. Electron interaction with matter has

some peculiarities because of its low mass and the moving electrons are identical with atomic electrons from which the greatest part of the energy of the particles is transferred under the decelerating action of Coulomb force (Tayal, 1992).

The energy-loss per unit path-length, -dE/dx, for a heavy particle with charge ze, moving at a velocity v << c is given by (Klimov, 1975):

$$-\frac{dE}{dx} = \frac{e^4}{4\pi\xi_o{}^2 m}\frac{z^2}{v^2} N Z \ln\frac{m v^2}{2 I \sqrt{e/2}} \qquad \text{-------(5.1)}$$

where,

m is the mass of the target material,

ξ_o is the permittivity of vacuum = 8.85×10^{-12} F/m,

NZ is the number of atoms per unit volume of the target material

$= \rho N_A (Z/A)$,

ρ is the density of the target material,

N_A is the Avagadro's number = 6.023×10^{23} mol^{-1},

A is the atomic weight of the target,

Z is the atomic number of the target,

I is the mean excitation energy of atoms of the medium $\approx$ 13Z eV.

Since energy-loss by ionisation varies approximately as $1/v^2$, –dE/dx is much smaller for electrons (whose velocity is higher for a

given energy) than for heavy particles at low and moderate energies (Ehrharat, 1984). Electrons with kinetic energy greater than 0.01 MeV are relativistic particles having low ionisation losses. The specific energy-loss by relativistic electrons is determined by the expression (Spinks and Woods, 1990):

$$-\frac{dE}{dx}=\frac{e^4 NZ}{8\pi\xi_o{}^2 m_e v^2}\left\{\ln\frac{m_o v^2 E}{2I^2(1-\beta^2)}-\left(2-\sqrt{1-\beta^2}-1+\beta^2\right)\times\ln 2+1-\beta^2+\frac{1}{8}\left(1-\sqrt{1-\beta^2}\right)^2\right\}$$

--------(5.2)

where,

E is the kinetic energy of the electron,

e is the elementary charge = 1.6 x 10^{-19} C,

m_o is the rest mass of the electron = 9.1 x 10^{-31} kg,

v is the velocity of the electrons,

β is v/c,

c is the velocity of light,

Z is the atomic number of the stopping material.

At lower velocities, β→0, this relation reduces to eqn. (5.1)

When v→c, β→1,

$$-\frac{dE}{dx}=\frac{e^4 NZ}{8\pi\xi_o{}^2 m_o c^2}\left(\ln\frac{E^3}{2m_o c^2 I^2}+\frac{1}{8}\right)$$

---------(5.3)

Energy-loss by emission of radiation is dominant for high energy electrons (>1 MeV). These radiative losses take the form of 'Bremsstrahlung' or braking electromagnetic radiation, which can emanate from any position along the electron track. An electron passing by the target nucleus experiences a Coulomb force and is deflected. The deceleration of the charged particle results in the emission of electromagnetic radiation known as 'Bremsstrahlung' (Sorensen, 1996). Thus, slowing down of electron in the nuclear field is accompanied by the emission of γ-rays with energy equal to the energy lost by the electron and can be any value down to the value of the initial kinetic energy of the electron. The probability of energy emission during the heavy ion interaction is 10^6 to 10^7 times lower than during electron deceleration. Bremsstrahlung is an important means of energy-loss only for electrons where $(z/m_e)^2 \approx 3\text{x}10^6$, with z and m_e being the charge and mass respectively of the incident electron.

The intensity of Bremsstrahlung at a given energy of the incident particle is directly proportional to $(z/m_e)^2 Z^2$, where Z is the charge of the target nucleus. Thus, in heavy materials such as Lead (Pb), the radiation loss becomes appreciable even at 1 MeV.

The probability of emission of Bremsstrahlung increases with energy of the electron beam. Bremsstrahlung predominates over ionisation at high energies and in heavy substances. Total linear stopping power for electrons is the sum of the collisional and radiative losses. The ratio of energy-loss by radiation to energy-loss by ionisation in an element of atomic number Z is approximately equal to EZ/800, i.e.,

$$\frac{\left(\frac{dE}{dx}\right)_{bremsstrahlung}}{\left(\frac{dE}{dx}\right)_{ionisation}} \cong \frac{EZ}{800} \qquad \text{---------(5.4)}$$

In lead, the rate of energy-loss by bremsstrahlung becomes equal to that by ionisation for electron of energy ~10 MeV, whereas in air bremsstrahlung remains small until electron energy reaches above ~100 MeV.

In the present work, the effect of 2 MeV electrons on Polyallyl diglycol carbonate (PADC), passing through three different metal targets viz. Lead, Gold and Molybdenum was studied.

5.2. EXPERIMENTAL ASPECTS

5.2.1. *Preparation of the target stacks*

PADC samples (composition: $C_{12}H_{18}O_7$, density: 1.32 g.cm^{-3}) of sizes (2x2) cm^2 were cut from commercially available sheets (thickness $\approx$ 1.5 mm), manufactured by Homalite Corporation, Wilmington, Del. (USA). After removing the surface protective layers, these detector plates were washed thoroughly with soap solution and then with deionised water to remove surface contamination. The cleaned samples were then dried inside a vacuum desiccator.

Three different types of metal foils were used for preparing the target stack. These were Lead foils (Z = 82, Thickness: 125 μm, density: 1.35 g.cm^{-3}), Gold foils (Z = 79, Thickness: 3 μm, density: 9.32 g.cm^{-3}) and Molybdenum foils (Z = 42, Thickness: 25 μm, density: 10.22 g.cm^{-3}). The target stacks were prepared placing six metal foils and five PADC samples alternately as shown in Fig. 5.1. For three metal foils three different target stacks were prepared.

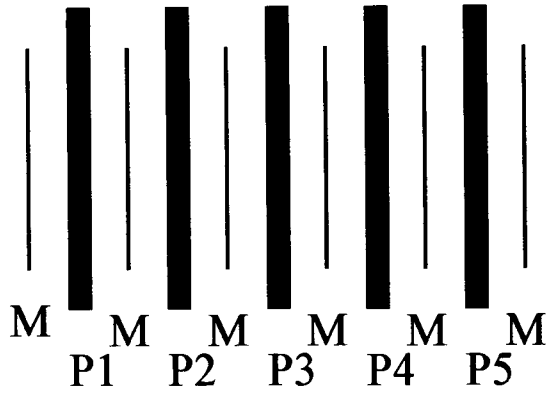

Fig. 5.1. Arrangement of metal foils (M) and PADC samples (P1, P2, P3, P4, P5) for each target stack.

5.2.2. *Irradiation and cooling*

Irradiation of the target stacks was done by a 23 kGy dose of 2 MeV electron beam from an electron generator at the Hahn-Meitner Institute, Berlin. The electron beam was allowed to pass through a collimator and was allowed to fall on the target stack placed at a distance of 2 metres from the collimator. Irradiated samples were allowed to cool for about 24 hours. The stacks were then taken and preserved in plastic boxes.

5.2.3. *Exposure to fission fragments*

The PADC samples were separated from the target stacks and small pieces of three PADC samples (P1, P3, P5) of each stack were further exposed to fission fragments from a ^{252}Cf source having a fission

activity of 5.7×10^3 s^{-1}. The PADC samples were mounted on a perspex holder kept at a distance of 1 cm from the source ^{252}Cf and exposed at an angle of 90°. An unstacked electron irradiated PADC was taken as pristine and it was also exposed to fission fragments in a similar manner. After irradiation, the samples were allowed to cool and then were stored in plastic boxes.

5.2.4. *Chemical treatment*

The samples were washed thoroughly in lukewarm soap solution to avoid non-uniformity in etching due to surface contamination. Then the cleaned samples were etched in 6N NaOH solution at an etching temperature of 55°C. Successive etching was performed till the tracks were completely etched. After every etching, the samples were washed in running water and dried in vacuum.

5.2.5. *Measurement of track parameters*

The track diameters of fission fragments were measured by Leitz optical microscope at a magnification of 625x. The bulk etch-rate (V_G) was calculated from the slope of the plot between normally incident fission-fragment track diameters (D_{ff}) versus etching time (t), using the track diameter method:

$$V_G = D_{ff} / 2t \qquad \text{.....(5.5)}$$

The error associated with the etch-rate measurements is ± 0.4 μm/h.

5.2.6. *Thermal analysis*

A simple automatic Perkin Elmer instrument was used for the thermal analysis of the 1st, 3rd and 5th PADC samples of each stack. The scanning rate for this instrument was adjusted to 20°C/min with nitrogen as flushing gas. The samples were crimped in small aluminium pans, weighed in a thermobalance and were scanned in the temperature range from 30°C to 600°C. The study of thermal stability was done with the help of thermogram, i.e., a plot of mass percent as a function of temperature which was obtained by the Perkin Elmer instrument. The error associated in recording the thermograms is ± 2°C.

5.3. RESULTS AND DISCUSSION

During the transition from one layer to another the cross-sections of electron scattering changes abruptly and the characteristics of electrons, both transmitted and reflected, depends upon the chemical composition of the layers (Balashov, 1999; Idoeta, 2000). The passage of electrons through the metallic target is accompanied by scattering and absorption, owing to the energy losses in collisions. The depth-dose distribution arises as a consequence of two processes:

energy-loss due to ionisation and excitation of target atoms and multiple scattering of electrons in the target. The stopping power depends on the atomic number and atomic weight of the target material. Both scattering and slowing down of electrons increase with increasing target-atom mass. The transmission coefficient of electrons for a target made of heavy atoms is less than for a target consisting of light atoms. The energy spectra of the transmitted electrons vary from almost Gaussian for small target thicknesses to a broad assymetric curve for large thicknesses. For the targets consisting of lighter atoms the number of low energy electrons in the spectrum decreases owing to reduction in generation of secondary electrons and weaker scattering. The maximum energy of the spectrum decreases too. The reflection coefficient is influenced both by a single large angle scattering and by multiple small angle scatterings. The heavier the target atoms, the higher is the number of singly scattered electrons. The reflected intensity increases with increasing thickness of the reflector except that for thickness greater than about one-third of the range of the electrons, saturation is achieved and further increase in thickness does not add to the reflected intensity. For generation of bremsstrahlung, the targets with high atomic number are used as a rule due to rapid increase of production cross-section with target

atomic number. The efficiency of conversion of kinetic energy to bremsstrahlung increases with increasing electron energy and with increasing charge of the target. Moreover, if thickness of the heavy layer increases, the emission coefficient of bremsstrahlung grows.

The electrons with kinetic energy 2 MeV are already relativistic. Ionisation-loss constitute the basic energy-loss mechanism of electrons moving with energy less than 10 MeV.

ENERGY-LOSS CALCULATION FOR LEAD

From eqn. (5.3), the energy-loss for lead can be derived as:

For Lead, $\frac{e^4 NZ}{8\pi\xi^2 mc^2} = 1.1 \text{ x } 10^{-11}\text{kg.m/s}^2$, $\left(\ln\frac{E^3}{2mc^2 I^2}+\frac{1}{8}\right) = -7.1577.$

Specific energy-loss by ionisation for lead was calculated to be,

$$-\frac{dE}{dx}=\frac{e^4 NZ}{8\pi\xi^2 mc^2}\left(\ln\frac{E^3}{2mc^2 I^2}+\frac{1}{8}\right) = -7.8735 \text{ x } 10^{-11} \text{ kg.m/s}^2.$$

Energy-loss by ionisation in lead foil of (125 μm) = 0.062 MeV.

Energy-loss by radiation of lead foil calculated from eqn.(5.4) was found to be approximately equal to 0.001 MeV.

ENERGY-LOSS CALCULATION FOR MOLYBDENUM

Similarly for Molybdenum, using eqn. (5.3) we get,

$$\frac{e^4 NZ}{8\pi\xi^2 mc^2} = 1.096 \text{ x } 10^{-11}\text{kg.m/s}^2, \left(\ln\frac{E^3}{2mc^2 I^2}+\frac{1}{8}\right) = -5.82.$$

Specific energy-loss by ionisation for Molybdenum was calculated to

be, $-\frac{dE}{dx}=\frac{e^4 NZ}{8\pi\xi^2 mc^2}\left(\ln\frac{E^3}{2mc^2 I^2}+\frac{1}{8}\right) = -6.379 \times 10^{-11}$ kg.m/s^2.

Energy-loss by ionisation in Molybdenum foil (25 μm) = 0.01 MeV.

Energy-loss by radiation by Molybdenum foil was found to be approximately equal to 0.0001 MeV.

ENERGY-LOSS CALCULATION FOR GOLD

For Gold, $\frac{e^4 NZ}{8\pi\xi^2 mc^2} = 1.898 \times 10^{-11}$kg.m/s^2, $\left(\ln\frac{E^3}{2mc^2 I^2}+\frac{1}{8}\right) = -7.085$.

Specific energy-loss by ionisation for Gold foil was calculated to be,

$-\frac{dE}{dx}=\frac{e^4 NZ}{8\pi\xi^2 mc^2}\left(\ln\frac{E^3}{2mc^2 I^2}+\frac{1}{8}\right) = -13.447 \times 10^{-11}$ kg.m/s^2.

Energy-loss by ionisation in Gold foil (3 μm) = 0.002 MeV.

Energy-loss by radiation of Gold foil was found to be approximately equal to 0.0003 MeV.

All the energy-loss data calculated for the three metallic foils is tabulated in Table 5.1. Total energy-loss is the sum of the energy loss by ionisation and that by radiation. As evident from the calculated energy-loss values, the maximum energy loss of 2 MeV electron has taken place when it passes through the lead foil. It is quite clear that, the energy-loss of the electron beam depends on the thickness of the

metallic foil. Owing to less thickness of the Gold foil, the energy-loss of electron beam was found to be low. The track diameters of the fission fragments from ^{252}Cf source in the PADC samples of the three stacks are tabulated in Table 5.2. The fission fragment track diameters in stacked PADC samples were found to be less than that in pristine PADC because in stacked PADC samples the amount of energy reaching the PADC samples was reduced due to energy-loss of electron.

Table 5.1. Energy-loss data calculated for 2 MeV electron beam passing through different metallic foils.

Metallic foil, Thickness (μm), and density ($g.cm^{-3}$)	Energy-loss by ionisation (MeV)	Energy-loss by bremsstrahlung (MeV)	Total energy-loss (MeV)
Lead, 125, 11.35	6.2×10^{-2}	0.1×10^{-2}	6.3×10^{-2}
Molybdenum, 25, 10.22	1.0×10^{-2}	0.01×10^{-2}	1.01×10^{-2}
Gold, 3, 19.32	0.2×10^{-2}	0.03×10^{-2}	0.23×10^{-2}

Table 5.2. Fission fragment track diameters in 1st (P1), 3rd (P3) and 5th (P5) PADC samples of the Lead, Molybdenum and Gold stack and that in pristine PADC.

Etching time (hours)	Fission fragment track diameters (μm)									
	Pristine	Lead stack			Molybdenum stack			Gold stack		
		P1	P3	P5	P1	P3	P5	P1	P3	P5
1.0	5.3	2.7	2.7	2.7	3.6	2.7	2.7	3.6	3.6	2.7
2.0	8.9	5.3	4.9	4.6	6.2	5.6	4.8	7.1	6.2	5.3
2.5	10.7	7.1	6.4	5.8	8.5	7.5	6.3	9.2	8.2	7.6
3.0	12.8	9.2	7.8	7.1	10.0	9.1	8.1	11.3	9.7	8.4
3.5	15.2	10.8	9.2	8.5	12.0	10.9	9.1	13.2	11.9	10.2

Among the stacked PADC samples, the track diameters were found to be maximum in the PADC of Gold stack because the energy loss by electrons was minimum for Gold foils. Thus, maximum energy has reached the PADC samples of Gold stack, resulting in increasing the bulk etch-rate probably due to chain-scission in PADC, as explained in Chapter 4. Again among all the PADC samples of the Gold stack, the diameters were found to be maximum in the 1st PADC

(P1) and were found to be gradually decreasing for 3rd and 5th PADC. The track diameters were found to be minimum for the PADC samples of the Lead stack because energy-loss was maximum in Lead foil. The track diameters in the 1st, 3rd and 5th PADC of all the stacks are shown in Fig. 5.2. The bulk etch-rate was calculated by using eqn. (5.5) and is tabulated in Table 5.3. The bulk etch-rate of pristine (stackless) PADC was found to be maximum, i.e., 2.2 μm/h.

Table 5.3. Variation of bulk etch-rate (V_G) of pristine along with the irradiated PADC samples (P1, P3, P5).

Sample	V_G (μm/h)
Pristine PADC (electron irradiated unstacked PADC)	2.2
P1 of Lead stack	1.5
P3 of Lead stack	1.3
P5 of Lead stack	1.2
P1 of Molybdenum stack	1.7
P3 of Molybdenum stack	1.5
P5 of Molybdenum stack	1.3
P1 of Gold stack	1.9
P3 of Gold stack	1.6
P5 of Gold stack	1.4

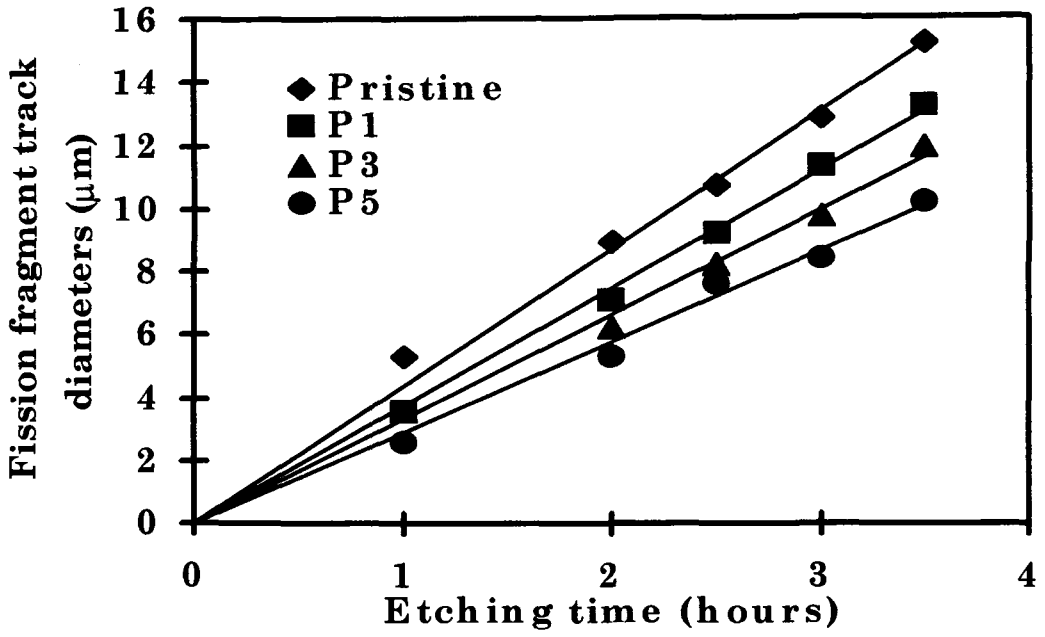

(I)

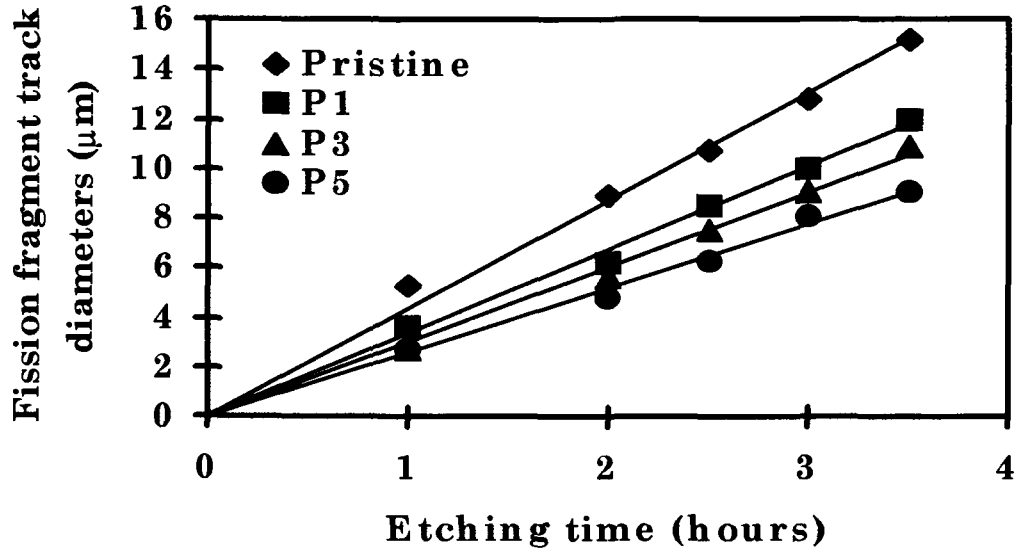

(II)

Fig. 5.2. The plot of fission track diameters versus etching time in 1st (P1), 3rd (P3) and 5th (P5) PADC samples along with the pristine PADC in
(I) Gold stack and (II) Molybdenum stack

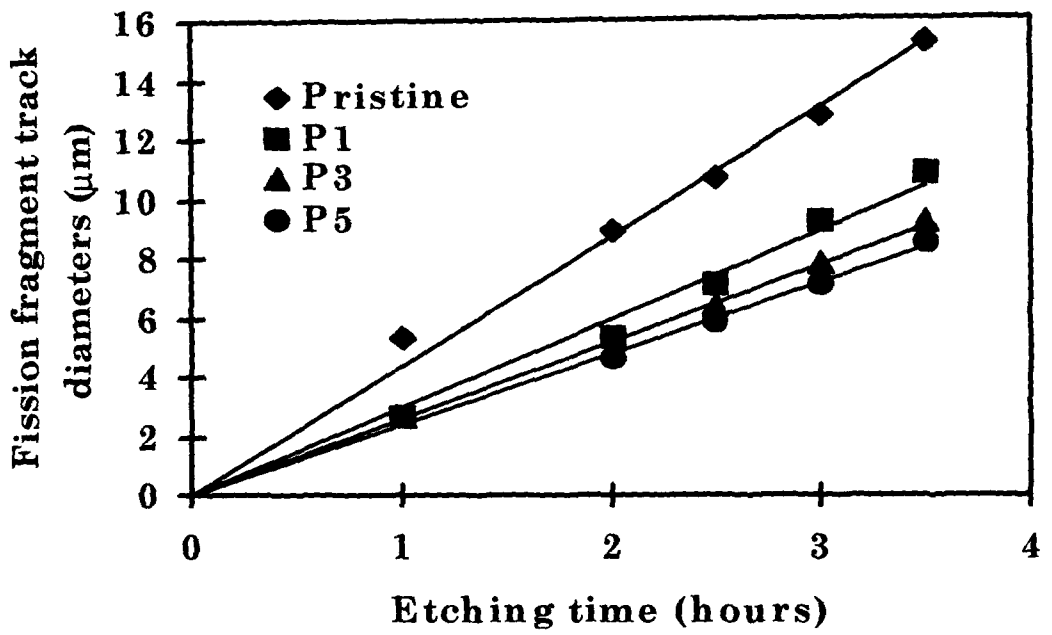

(III)

Fig. 5.2. The plot of fission track diameters versus etching time in 1st (P1), 3rd (P3) and 5th (P5) PADC samples along with the pristine PADC in (III) Lead stack

Among the stacked PADC samples, the maximum bulk etch-rate was found to be 1.9 μm/h for 1st PADC of Gold stack and the minimum was found to be 1.2 μm/h for 5th PADC of Lead stack. The energy-loss of electrons through Lead foil was maximum resulting in minimum bulk etch-rate. Thermal analysis of the samples showed that the pristine PADC was most stable. The pristine (stackless) PADC remained stable from up to 93°C. The 1st PADC (P1) of Gold stack was

least stable among all the stacked PADC samples. The bulk etch-rate of this PADC was maximum. This implied that the chain-scission mechanism is more prominent in this PADC, which in turn, indicated that more electron energy was incident on the sample.

In each stack, thermal stability increased with increase in the penetration depth of the electrons. The last PADC sample in each stack was most stable denoting that less energy was deposited in this sample. The data for the stable zone of all the samples have been compiled in Table 5.4. The thermograms for the 1st PADC samples of all the three stacks are shown in Fig. 5.3.

As it is evident from the thermogram that, due to maximum energy-loss by electrons for Lead, minimum electron energy was deposited on the 1st PADC of Lead stack in comparison to 1st PADC samples of other two stacks. So, the extent of chain-scission (as a function of the deposited energy) seems to be less in this sample (1st PADC of Lead stack), thus leading to its more stability than that of the 1st PADC samples of the other stacks.

Table 5.4. Thermal stability of the pristine PADC (P) along with that of the PADC samples (1st: P1, 3rd : P3 and 5th: P5) of different stacks.

Stack	Sample	Thermal Stability(°C)
---	Pristine (P)	30 - 93
Lead	P1	30 - 107
	P3	30 - 125
	P5	30 - 131
Molybdenum	P1	30 - 100
	P3	30 - 125
	P5	30 - 131
Gold	P1	30 - 95
	P3	30 - 122
	P5	30 - 130

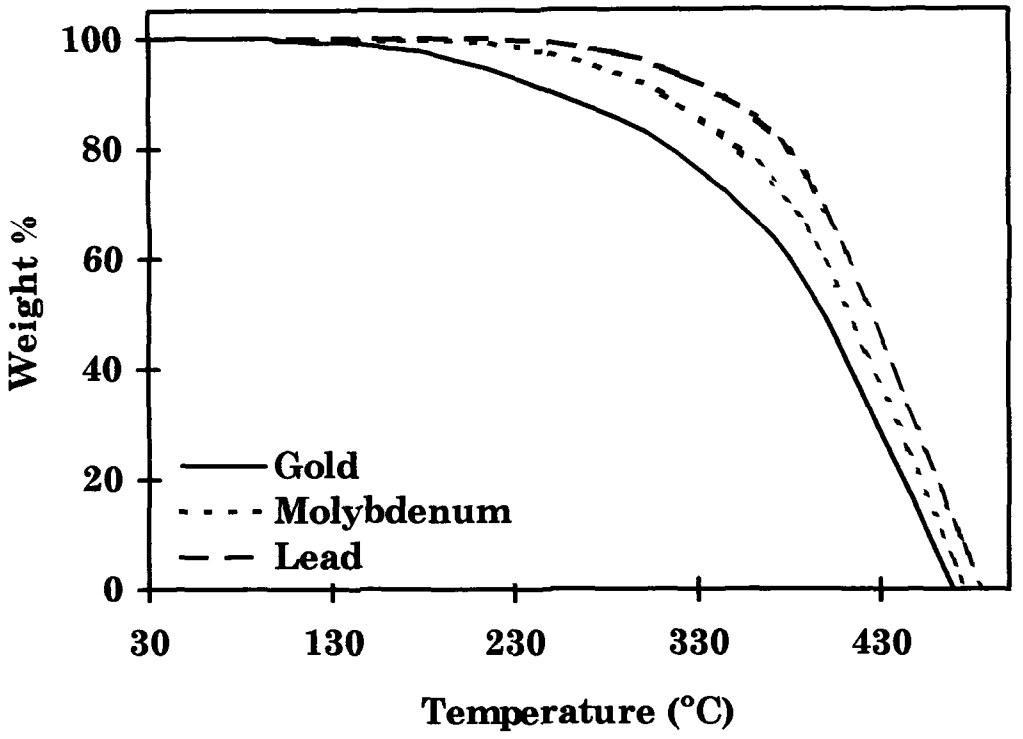

Fig. 5.3. The thermograms of the 1st PADC samples of all the three stacks (Gold, Molybdenum and Lead), showing their thermal decomposition behaviour.

5.4. CONCLUSION

2 MeV electrons, while traversing through a material medium loses energy through ionisation and radiative emission. The total energy-loss by the electron beam is the sum of the ionisation and radiation energy-loss. The energy-loss by electrons was found to be

dependent on the charge, mass, thickness and density of the target material. The energy-loss by electrons was found to be high for Lead foil because of its large atomic number and thickness. The energy-loss of electron while traversed through the Molybdenum foil was found to be more than the energy-loss, when it passed through Gold foil because, though the density and atomic number of Gold foil was more than that of Molybdenum, yet the thickness of the Gold foil was only 3μm. These results were further confirmed by track studies and thermogravimetric analysis. The fission track diameters in the 1st PADC samples of each stack were observed to be more than that in other PADC samples of the same stack. This is due to gradual energy-loss of the electron beam as it traverses deeper through the stack. The maximum energy was deposited in the 1st PADC samples of each stack and hence, the effect of chain-scissioning was relatively more, which resulted in faster bulk etch-rate. Among the 1st PADC samples of all the three stacks, the PADC of Gold stack was found to be having the highest bulk etch-rate due to minimum energy-loss of electron beam while passing through the Gold foil. The bulk etch-rate of the PADC of Lead stack was found to be minimum because of the maximum energy-loss by electron while traversing through the Lead foil. The thermal analysis of the PADC sample showed that the PADC

of Lead stack was comparatively more stable. This might be due to less energy deposition by the electrons, on the PADC sample because of maximum energy-loss of electron through the Lead foil. So, the PADC of the Lead stack is comparatively more thermally stable than the PADC samples of other two stacks.